Influence of parent vessel dominancy on fluid dynamics of anterior communicating artery aneurysms

Acta Neurochirurgica
The European Journal of Neurosurgery

ISSN 0001-6268
Volume 153
Number 2

Acta Neurochir (2010)
153:305-310
DOI 10.1007/
s00701-010-0824-1

Springer

Acta Neurochir (2011) 153:305–310
DOI 10.1007/s00701-010-0824-1

EXPERIMENTAL RESEARCH

Influence of parent vessel dominancy on fluid dynamics of anterior communicating artery aneurysms

Tamer Hassan · Amr Ali Hassan · Yaser Mohamed Ahmed

Received: 6 August 2010 / Accepted: 23 September 2010 / Published online: 6 October 2010

Abstract
Background Parent vessel plays an important role in aneurysm formation and rupture. The diameter of either the A1 arteries is the peculiar key controlling the flow of the anterior communicating artery (ACOMA) aneurysms (ANs).
Objective The purpose is to study the effect of parent vessel dominancy, that is, the diameter of the A1 artery, on the flow characteristics of the ACOMA ANs.
Methods Numerical simulations for the flow patterns in six artificial models have been studied. Three models are designed with aneurysms and three models without. The two A1s were equal in two models. In the other two models, the nondominant A1 diameters were decreased by 50%. Again, the nondominant A1s were decreased by another 50% in the last two models. Each pair was designed with and without aneurysms in the ACOMA.
Findings The ACOMA shows lower velocity magnitudes and wall shear stresses when the two A1s are equal. However, if one A1 is dominant with a 50% difference from the other A1, there is higher shear stress on the ACOMA itself and in the inflow zone of the aneurysm that increases more with further reduction of the nondominant A1 by another 50%. An area of high corner pressure at the bifurcation of the dominant A1 into the ACOMA and A2 exists and increases in value with the decrease of diameter of the other nondominant A1.
Conclusion Aneurysms located in the ACOMA with differences of 50% or more between the two A1s are subjected to more flow stresses.

Keywords Fluid dynamics · Aneurysm · Parent vessel · A1 · Anterior communicating artery

T. Hassan (✉)
Department of Neurosurgery,
Alexandria University School of Medicine,
Elazarita, Shambeleon Street,
Alexandria, Egypt
e-mail: Neurocatheter@yahoo.com

T. Hassan
e-mail: Thassan@aast.edu

A. A. Hassan
Marine Engineering Department, College of Engineering,
Arab Academy for Science,
Technology and Maritime Transport (AASTMT),
Alexandria, Egypt

Y. M. Ahmed
Department of Naval Architecture and Marine Engineering,
Faculty of Engineering, Alexandria University,
Alexandria, Egypt

Introduction

Anterior communicating artery (ACOMA) complex is the most frequent site of ruptured intracranial aneurysms (ANs) in most reported series [1]. ACOMA ANs are the most complex ANs of the anterior circulation due to their complex angioarchitecture and the special flow dynamics of the ACOMA region. ACOMA acts as a communication between the two A1 arteries that are variable in their diameter among different populations. ACOMA ANs are more prone to rupture and demonstrate the highest incidence of postoperative morbidity among anterior circulation ANs [5].

Blood flow dynamics are thought to be an important factor in the pathogenesis and treatment of cerebral ANs [2, 6]. A number of specific hemodynamic factors—notably wall shear stress, pressure stress, impingement force, flow

rate, and residence time—have been implicated in aneurysm growth and rupture [3, 16].

Numerical flow simulations have been performed in different research studies on simple models of intracranial ANs as well as real models obtained from 3D angiography images [7, 9, 10]. The effect of changes of the neck diameter and size of the parent vessels have been studied before [8, 18]. The present study is focused on the effect of change of the diameter of one A1 vessel on the hemodynamic pattern of the ACOMA. The study aimed at describing the variation of wall shear stresses, pressures, and the velocity patterns among different patterns of dominancy at the ACOMA complex.

Methods

Grid generator

Figure 1 illustrates the different models of the ACOMA complexes with and without ANs. The diameters of the vessels are explained in the Fig. 1 legend. Volume grid generation was performed using the grid generator of the finite-volume code Fluent (Fluent Inc., Lebanon, NH) to build 3D unstructured tetrahedral models. The Mesh Editor and Tetra tools have been used to define the inlets, the outlets, and the wall boundaries of the computational domains. Mesh smoothing further improved the grid quality. The numbers of unstructured tetrahedral mesh elements in the grids used to compute the cases presented in Fig. 1 were within the range 28,619–31,945.

Flow modeling

The continuity equation for mass conservation and the 3D incompressible Navier–Stokes equations for momentum transport equations were used for blood flow simulations. Blood is usually considered a Newtonian fluid; this is a fairly good approximation for large-bore vessels. The simulations used in the present study were performed with the following fluid properties: blood density 1,060 kg/m^3 and blood dynamic viscosity 0.004 Poiseuille.

The rigid vessel assumption was considered in this study. Under this, any computational flow dynamics (CFD) code with incompressible fluid modeling capabilities can be used. In the code, the governing equations written in conservative form for mass and momentum were discretized with a finite-volume method. The SIMPLE (Semi-

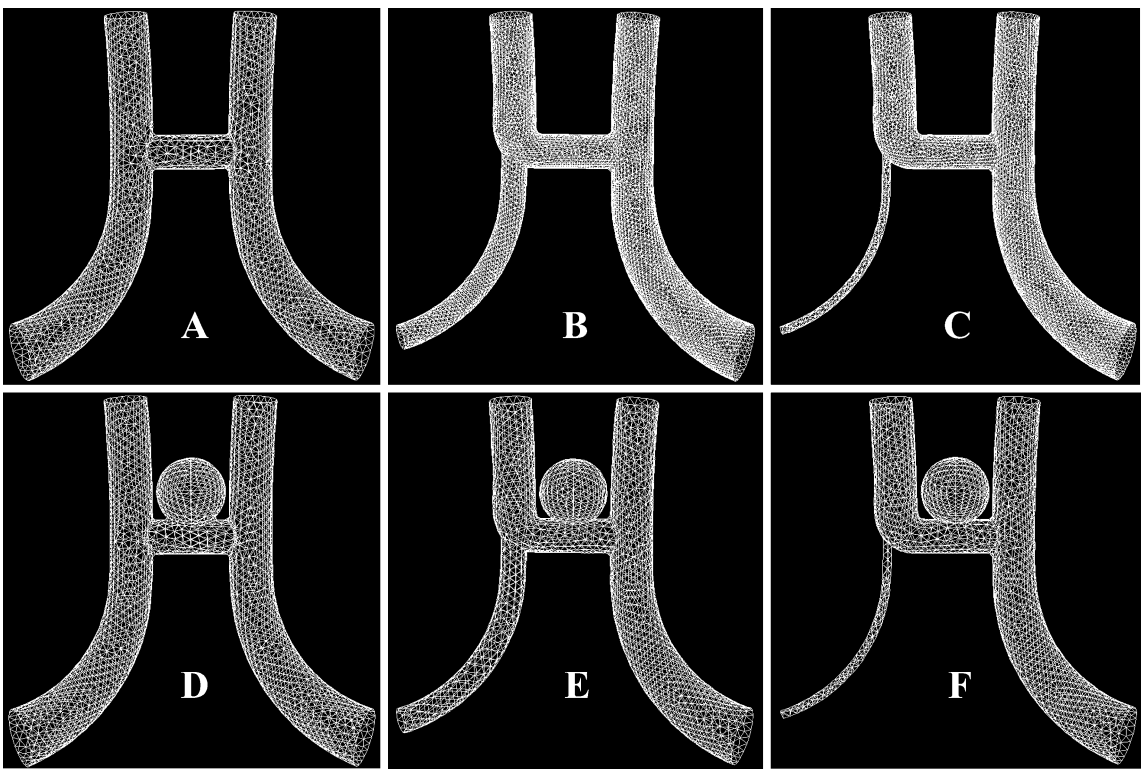

Fig. 1 Schematic drawing for the unstructured tetrahedral grids representing the six vascular models. **a** and **d** demonstrate the ACOMA geometry with equal A1 arteries (3.5 mm at inflow (A1); 2.5 mm at outflow (A2)) with (**d**) and without aneurysm (**a**). **b** and **e** demonstrate the ACOMA geometry with unequal A1 arteries (50% decrease of the left A1 than **a** and **d**; 1.5 mm) with (**b**) and without (**e**) aneurysm. **c** and **f** demonstrate the ACOMA geometry with unequal A1 arteries (50% decrease of the left A1 than **b** and **e**; 0.75 mm) with (**f**) and without (**c**) aneurysm. Aneurysm and ACOM artery diameters were both set at 4 mm

Implicit Methods for Pressure-Linked Equations) method to solve the discretized equations is used [9]. To improve the convergence speed, under-relaxation factors were applied to velocity and pressure modifications. On the rigid vessel walls, the nonslip condition was used. For the outlet, the outflow boundary condition was used. The blood flow was assumed to be a steady, laminar, incompressible fluid. The governing equations for blood flow can be written in Cartesian form as follows:

$$\nabla \cdot \vec{u} = 0 \tag{1}$$

$$\left(\vec{u} \cdot \nabla\right)\vec{u} = -\frac{\nabla p}{\rho} + \nu\nabla^2\vec{u} \tag{2}$$

The blood vessel walls of the different cases were treated as rigid viscous walls with no slip boundary condition. Uniform flow conditions at the inlet and exit planes were applied. Blood was modeled to have a velocity of 80 ml/min at the inlets [20]. The algebraic equations obtained from the discretization process are solved iteratively. Solution convergence was monitored by dimensionless residual sum for all variables across the computational points. The residual absolute criteria were set to the value of 0.001 for checking the convergence of the solution.

Results

Figure 2 illustrates the velocity patterns, the wall shear stresses, and the pressures for the different six cases. If the two A1s are equal (cases A and D), the ACOMA shows lower values for velocity magnitude in comparison with those values measured in the A1 and A2 arteries. Consequently, the shear stresses on the ACOMA wall will be also low, and accordingly, the ANs located in the ACOMA with equal A1s are subjected to the least wall shear and flow dynamic stresses.

However, if one A1 is dominant with 50% differences (cases B and E), the differences in size between A1 and A2 arteries cause the formation of high pressure area at the intersection between the dominant A1, A2, and ACOM arteries. Furthermore, there is a noticeable flow jet starting from the dominant A1 and directed into the ACOMA. This flow jet accelerates the blood flow in the ACOMA, especially on its aneurysmal side with a consequent increase in wall shear stresses on this region and at the inflow zone of the aneurysm.

Further reduction of the nondominant A1 by 50% (cases C and F) leads to higher pressures at the dominant A1, A2, and ACOMA corner junction in addition to higher shear stresses on the ACOMA itself and in the inflow zone of the aneurysm.

Figure 3 demonstrates the changes in corner pressure in cases D, E, F. The corner pressure located at the bifurcation of the dominant A1 into ACOMA and A2 increases with the decrease of diameter of the nondominant A1. Wall shear stresses calculated at the aneurysmal inflow zone increase with the decrease in the diameter of the nondominant A1, reflecting a higher jet flow speed inside the aneurysmal inflow zone; this high jet implies decrease in intra-aneurysmal inflow zone pressures as shown in the same figure.

Discussion

The physiological mechanisms that give rise to the inception and development of a cerebral aneurysm are accepted to involve the interplay between the local mechanical forces acting on the arterial wall and the biological processes occurring at the cellular level. Little is known about the biological mechanisms associated with the genesis, growth, and rupture of intracranial saccular aneurysms. It is postulated that the vascular wall pathological response of aneurysmal disease is associated with abnormal angiogenesis factor expression as well as proteolysis. Vascular endothelial growth factor is known to be a regulator of angiogenesis and to simultaneously stimulate elastolytic proteinases [15]. Nishibe et al. clearly demonstrated the expression of this factor in endothelial cells, smooth muscle cells, and macrophages of abdominal aortic aneurysms as well as its absence in those cells of normal abdominal aorta, suggesting that vascular endothelial growth factor may play an important role in aneurysm formation [13]. The external triggers linked to the brain environment or precisely peri-aneurysmal environment (subarachnoid space, cerebral cortex) may also play an active part in the creation and morphology of aneurysms [19].

Patient-specific blood flow simulations provide an attractive method for the study of intra-aneurysmal hemodynamics because of the ability to study all the possible geometries. Although complex real aneurysmal models bring us closer to real patient problems, the simplified geometries provide a basic understanding of the flow and allow the study of the influence of certain geometrical parameters with higher accuracy and controllability compared to the infinite variety of shapes and very complex flow patterns from real aneurysmal models. The present study aims to prove through CFD the effect of change of the diameter of one A1 vessel on the hemodynamic pattern of the ACOMA complex. In this discussion, the question is "Do ANs grow at high pressure zones on curves and at bifurcation points and then continue to grow and enlarge because of high shear stresses?!"

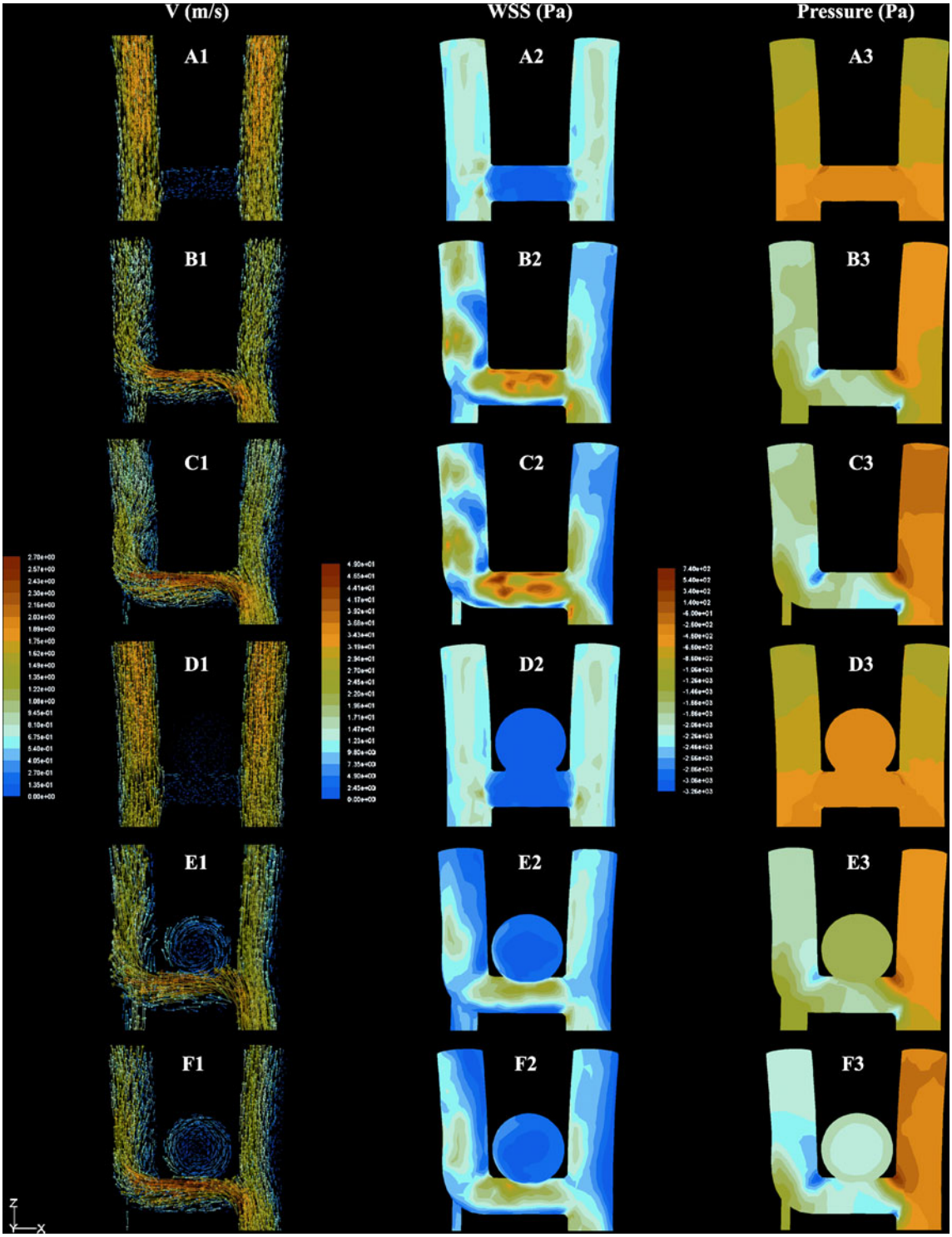

Fig. 2 Velocity, wall shear stresses, and pressure results for all geometries. *Left column* (*A1–F1*) demonstrates typical instant streamlines colored by velocity (meters per second) that shows that the blood stream velocity increases more in the ACOMA and aneurysm with the decrease in the diameter of the nondominant A1 (*C1>B1>A1*, *F1>E1>D1*). *Middle column* (*A2–F2*) demonstrates typical instant wall shear stress distribution (Pascal) that shows highest local shear stresses in the ACOMA (*C2*) and in the inflow zone of the aneurysm (*F2*) with the least diameter of the nondominant A1. *Right column* (*A3–F3*) demonstrates typical instant surface pressure (Pascal) for the entire geometries showing a high pressure corner area (*red*) on the wall opposite to the bifurcation of the A1 into A2 and ACOMA that does not exist with the equal A1 cases (*A3*, *D3*). This high pressure area increases in value with the decrease of A1 diameter (*F3>E3*, *C3>B3*). The locally higher normal pressure may lead to subsequent growth of the aneurysm at this corner location

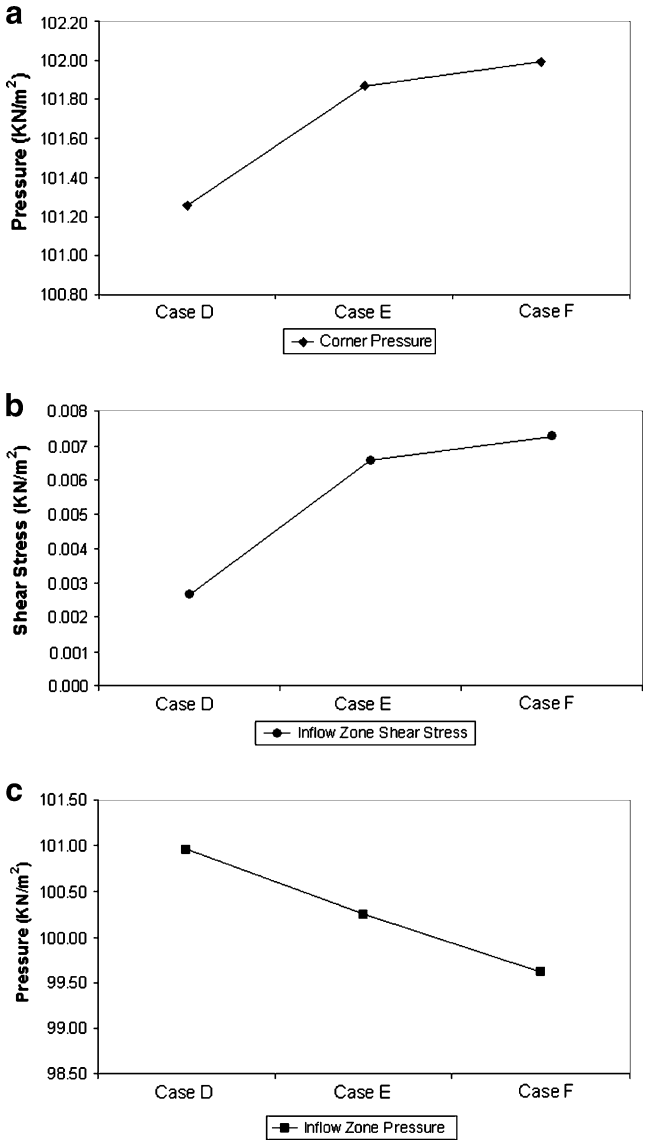

Fig. 3 Three line diagrams (**a**, **b**, **c**). Graph **a** demonstrates the changes in corner pressure between cases **d**, **e**, and **f**. The corner pressure located at the bifurcation of the dominant A1 into ACOMA and A2 increases with the decrease of diameter of the other nondominant A1. Graph **b** demonstrates the changes in the aneurysmal inflow zone shear stresses that increase more with the decrease in the diameter of the nondominant A1, reflecting higher jet flow speed inside the aneurysmal inflow zone that implies a decrease in intra-aneurysmal inflow zone pressures as shown in graph **c**. Shear stress values were taken from a fixed point at the inflow zone of the aneurysm

ACOMA ANs are the most common ruptured ANs in neurosurgical practice. They are commonly found at the A1–A2 junction on the dominant side. The angle of the arteries at the bifurcation and the direction of blood flow are factors of hemodynamic stress in the apical region where these ANs often develop. They exist at the bifurcation of dominant A1, A2, and ACOMA and usually point in the direction away from the dominant A1 [1]. The growth of ACOMA aneurysm at this anatomic location matches that of the high pressure area located at the junction of the dominant A1, A2, and ACOMA in this study. Although a small pressure increase of 0.6 kN/m^2 was found at this junction area, this figure, in this limited simulation, is only a relative value within the respective geometry. The true figure may be of significance in the initiation of aneurysm growth at this junction area location.

This junction area was found to be the most likely among the other geographic areas of the ACOMA complex to harbor the formation of ACOMA aneurysm. Such risk increases with increasing differences in the blood flow percent in the two A1s. This difference may result from the actual difference in the A1 artery diameter or due to the variation in the blood flow between the two carotid arteries. Such location can anatomically be described as the bifurcation of the A1 into A2 and ACOMA. Several other research studies support the formation of ANs at high pressure areas facing the incoming flow jet of the blood stream [4, 6].

The present results qualitatively match that of Kerber et al. [12] who studied experimentally the flow dynamics of ruptured lethal ACOMA. When flow was bilaterally equal between the internal carotid artery (ICA), the anterior cerebral artery (ACA), and the middle cerebral artery (MCA), opacified fluid slipstreams did not enter the aneurysm. This flow state should not result in aneurysm growth or rupture and is highly unlikely to result in aneurysm formation. However, when flow was bilaterally asymmetrical between either the afferent ICA or the efferent ACA or MCA, opacified fluid slipstreams entered the aneurysm. This flow state should result in aneurysm growth and possible eventual rupture and may be a factor in aneurysm formation. Asymmetrical flow of the afferent ICA can be secondary to a fixed anatomic lesion, such as atherosclerotic carotid stenosis or, rarely, hypoplasia of the ICA. In addition, temporary blood flow alterations may occur during changes in body position, such as head turning. Asymmetrical flow of the efferent arteries can be secondary to anatomic anomalies, such as hypoplasia of the A1 segment of the anterior cerebral arteries, or from atherosclerosis of these vessels. The intra-aneurysmal flow was found to increase computationally with the decrease of the diameter of the nondominant A2, exposing the ACOMA and the aneurysm to more shear stresses that promote aneurysmal growth.

Wall shear stress is a dynamic frictional force induced by a viscous fluid moving across a surface of solid material. In recent investigations, it has been suggested that oscillating wall shear stress stimulates the release of endothelium-derived nitric oxide, which is known as a strong vasodilator and is also a potential factor in arterial wall degeneration

due to local destruction of extracellular matrix and host cell cytotoxic effects. Therefore, a local increase in the wall shear stress may cause local dilation and degeneration of arterial walls [4, 8, 17].

The hypothesis describing that fluid-induced wall shear stress would be of significance in initiation or growth of aneurysm is still not proved although several research studied the relationship between fluid-induced wall shear stress with aneurysm and bleb growth. The blebs facing the incoming blood flow at the inflow zones were found to be those at high risk for rupture [4, 8, 11, 14]. High-wall shear stress status necessitates the existence of a high-flow state, that is, wide necks or wide bore draining vessels [8] or a significant difference between A1 diameters as present. The larger the differences between A1 diameters, the higher the shear stresses at inflow zone and the larger the possibility that aneurysm will grow faster or rupture earlier.

The present increase of intra-aneurysmal blood flow and inflow zone shear stresses with the decrease of the diameter of the nondominant ACOMA may be of clinical value in anticipating the higher risk of rupture of a small non-ruptured ACOMA aneurysm with an atretic one A1, putting this patient under special consideration for early surgery or endovascular treatment. It also simplifies that aneurysms located on ACOMA with differences of 50% or more between the two A1s are subjected to more flow dynamic stresses. Further studies on real ACOMA ANs geometries are needed in correlation with patients' clinical data.

Conflicts of interest None.

References

1. Agrawal A, Kato Y, Karagiozov K, Yoneda M, Imizu S, Sano H, Kanno T (2008) Anterior communicating artery ANs: an overview. Minim Invasive Neurosurg 51(3):131–135
2. Castro MA, Putman CM, Sheridan M, Cebral JR (2009) Hemodynamic patterns of anterior communicating artery ANs: a possible association with rupture. AJNR Am J Neuroradiol 8:1–6
3. Cebral JR, Castro MA, Appanaboyina S (2005) Efficient pipeline for image-based patient-specific analysis of cerebral aneurysm hemodynamics: technique and sensitivity. IEEE Trans Med Imaging 24:457–467
4. Cebral JR, Sheridan M, Putman CM (2010) Hemodynamics and bleb formation in intracranial aneurysms. AJNR Am J Neuroradiol 31:304–310
5. Charbel FT, Seyfried D, Mehta B, Dujovny M, Ausman JI (1991) Dominant A1: angiographic and clinical correlations with anterior communicating artery ANs. Neurol Res 13(4):253–256
6. Hassan T, Ezura M, Timofeev EV, Tominaga T, Saito T, Takahashi A, Takayama K, Yoshimoto T (2004) Computational simulation of therapeutic parent artery occlusion to treat giant vertebrobasilar aneurysm. AJNR Am J Neuroradiol 25:63–68
7. Hassan T, Timofeev EV, Ezura M, Saito T, Takahashi A, Takayama K, Yoshimoto T (2003) Hemodynamic analysis of an adult vein of Galen aneurysm malformation by use of 3D image-based computational fluid dynamics. AJNR Am J Neuroradiol 24:1075–1082
8. Hassan T, Timofeev EV, Saito T, Shimizu H, Ezura M, Matsumoto Y, Takayama K, Tominaga T, Takahashi A (2005) A proposed parent vessel geometry–based categorization of saccular intracranial ANs: computational flow dynamics analysis of the risk factors for lesion rupture. J Neurosurg 103:662–680
9. Hassan T, Timofeev EV, Saito T, Shimizu H, Ezura M, Tominaga T, Takahashi A, Takayama K (2004) Computational replicas: anatomical reconstructions of cerebral vessels as volume numerical grids at three-dimensional angiography. AJNR Am J Neuroradiol 25:1356–1365
10. Karmonik C, Klucznik R, Benndorf G (2008) Comparison of velocity patterns in an AComA aneurysm measured with 2D phase contrast MRI and simulated with CFD. Technol Health Care 16(2):119–128
11. Karmonik C, Yen C, Grossman RG, Klucznik R, Benndorf G (2009) Intra-aneurysmal flow patterns and wall shear stresses calculated with computational flow dynamics in an anterior communicating artery ANs depend on knowledge of patient-specific inflow rates. Acta Neurochir Wein 151(5):479–485
12. Kerber CW, Imbesi SG, Knox K (1999) Flow dynamics in a lethal anterior communicating artery ANs. AJNR Am J Neuroradiol 20:2000–2003
13. Nishibe T, Dardik A, Kondo Y, Kudo F, Muto A, Nishi M, Nishibe M, Shigematsu H (2010) Expression and localization of vascular endothelial growth factor in normal abdominal aorta and abdominal aortic aneurysm. Int Angiol 29(3):260–265
14. Shojima M, Oshima M, Takagi K, Torii R, Nagata K, Shirouzu I, Morita A, Kirino T (2005) Role of bloodstream impacting force and the local pressure elevation in the rupture of cerebral ANs. Stroke 36:1933–1938
15. Skirgaudas M, Awad IA, Kim J, Rothbart D, Criscuolo G (1996) Expression of angiogenesis factors and selected vascular wall matrix proteins in intracranial saccular aneurysms. Neurosurgery 39(3):537–545, discussion 545–7
16. Steinman DA, Milner JS, Norley CJ, Lownie SP, Holdsworth DW (2003) Image-based computational simulation of flow dynamics in a giant intracranial aneurysm. AJNR Am J Neuroradiol 24:559–566
17. Tateshima S, Murayama Y, Villablanca JP, Morino T, Nomura K, Tanishita K, Vinuela F (2003) In vitro measurement of fluid-induced wall shear stress in unruptured aneurysms harboring blebs. Stroke 34:187–192
18. Ujiie H, Tamano Y, Sasaki K, Hori T (2001) Is the aspect ratio a reliable index for predicting the rupture of a saccular aneurysm? Neurosurgery 48:495–503
19. Watton PN, Raberger NB, Holzapfel GA, Ventikos Y (2009) Coupling the hemodynamic environment to the evolution of cerebral aneurysms: computational framework and numerical examples. J Biomech Eng 131(10):101003
20. Zhao M, Amin-Hanjani S, Ruland S, Curcio AP, Ostergren L, Charbel FT (2007) Regional cerebral blood flow using quantitative MR angiography. AJNR Am J Neuroradiol 28(8):1470–1473